Generation of Thiocillin Ring Size Variants by Prepeptide Gene Replacement and In Vivo Processing by Bacillus cereus.

Albert A. Bowers, Michael G. Acker, Travis S. Young, and Christopher T. Walsh
Department of Medicinal Chemistry and Molecular Pharmacology, Purdue University, West Lafayette, IN, 47907
Department of Biological Chemistry and Molecular Pharmacology, Harvard Medical School, Boston, Massachusetts 02115

Supporting Information

Contents:

I. Materials and General Methods

All molecular biology, recombinant DNA manipulation and microbiological assays were performed following the protocols of Sambrook *et al*.[1] Unless otherwise specified, all chemicals were purchased from Sigma-Aldrich. Restriction enzymes and Quick Ligase were purchased from New England Biolabs (Boston, MA). Pfu Turbo DNA Polymerase was purchased from Invitrogen (Carlsbad, CA) and Paq 5000 DNA polymerase from Stratagene (La Jolla, CA).DNA oligonucleotide primers were synthesized by Integrated DNA technologies (Coralville, IA). PCR was performed on a Biorad MyCycler thermal cycler. DNA sequencing was performed by the Molecular Biology Core Facilities at the Dana Farber Cancer Institute (Boston, MA). Top10 chemically competent *E. coli* cells were purchased from Invitrogen. Restriction endonuclease cleanup and gel extraction of DNA fragments were performed with QiaQuick PCR cleanup kit from Qiagen. Recombinant plasmids were isolated using the QiaPrep Spin Miniprep Kit from Qiagen. *B. cereus* ATCC 14579 genomic DNA was isolated from cultures using the DNeasy Kit from Qiagen. Extraction of thiocillins from cell-free media was performed on Sep-Pak C18 cartidges from Waters Corp. (Milford, MA). Preparative RP-HPLC was performed on a Beckman System Gold (Beckman Coulter) instrument using a Phenomenex Luna 10 μm C18(2) 100 Å 250 x 21.20 mm column, monitoring eluent absorption at 220 and 350 nm.

II. Mutagenesis of *tclE* in pMGA-tclE-KI

As previously described,[2] plasmid pMGA-tclE-KI was generated using pLW111[3] which contains ~1 kb of homology to *tclD*. Mutants of *tclE* were then generated by site-directed

mutagenesis of plasmid pMGA-tclE-KI using overlapping primer extension. Briefly, homologous primers were designed each containing the mutation of interest flanked by 15-20 bps of homologous plasmid DNA sequence. PCR was performed with Pfu Turbo to extend the primers, generating entire circular plasmid strands, each containing the mutation of interest. Restriction endonuclease DpnI was then added to the reaction. DpnI selectively cleaves the methylated template plasmid, having been purified from bacterial cultures, while leaving intact the unmethylated mutant plasmid generated by PCR. The resulting mixture was transformed into chemically competent *E. coli* TOP10 cells and positive transformants were selected for on LB agar supplemented with 100 µg/mL ampicillin. Plasmid DNA was purified and mutants were confirmed by DNA sequencing. pMGA-tclE mutant plasmids were transformed into our Δ*tclE-H* mutant strain of *B. cereus* and selected on lincomycin-erythromycin (MLS) resistance.[2]

SI Table II.1. Oligonucleotides used for cloning and *tclE* mutagenesis

Oligo	Sequence	Role
Primer 209	5'-GAA ATT ATG GGA GCG TCA TGT GCG ACA TGC GTA TGT ACA TGC AG-3'	G(3,4) mutagenesis
Primer 210	5'-CTG CAT GTA CAT ACG CAT GTC GCA CAT GAC GCT CCC ATA ATT TC-3'	G(3,4) mutagenesis
Primer 211	5'-GAA ATT ATG GGA GCG TCA TGT GCG ACA TGC GTA TGT ACA TGC AG-3'	GG(3,4) mutagenesis
Primer 212	5'-CTG CAT GTA CAT ACG CAT GTC GCA CAT GAC GCT CCC ATA ATT TC-3'	GG(3,4) mutagenesis
Primer 213	5'-GAA ATT ATG GGA GCG TCA TGT GCG ACA TGC GTA TGT ACA TGC AG-3'	GGG(3,4) mutagenesis
Primer 214	5'-CTG CAT GTA CAT ACG CAT GTC GCA CAT GAC GCT CCC ATA ATT TC-3'	GGG(3,4) mutagenesis
Primer 215	5'-GAA ATT ATG GGA GCG TCA TGT GCG ACA TGC GTA TGT ACA TGC AG-3'	ΔT3 mutagenesis
Primer 216	5'-CTG CAT GTA CAT ACG CAT GTC GCA CAT GAC GCT CCC ATA ATT TC-3'	ΔT3 mutagenesis
Primer 217	5'-GAA ATT ATG GGA GCG TCA TGT GCG ACA TGC GTA TGT ACA TGC AG-3'	S(1,2) mutagenesis
Primer 218	5'-CTG CAT GTA CAT ACG CAT GTC GCA CAT GAC GCT CCC ATA ATT TC-3'	S(1,2) mutagenesis
Primer 219	5'-GAA ATT ATG GGA GCG TCA TGT GCG ACA TGC GTA TGT ACA TGC AG-3'	C2S mutagenesis
Primer 220	5'-CTG CAT GTA CAT ACG CAT GTC GCA CAT GAC GCT CCC ATA ATT TC-3'	C2S mutagenesis
Primer 221	5'-GAA ATT ATG GGA GCG TCA TGT GCG ACA TGC GTA TGT ACA TGC AG-3'	C9S mutagenesis
Primer 222	5'-CTG CAT GTA CAT ACG CAT GTC GCA CAT GAC GCT CCC ATA ATT TC-3'	C9S mutagenesis
Primer 223	5'-GAA ATT ATG GGA GCG TCA TGT GCG ACA TGC GTA TGT ACA TGC AG-3'	S(9,10) mutagenesis
Primer 224	5'-CTG CAT GTA CAT ACG CAT GTC GCA CAT GAC GCT CCC ATA ATT TC-3'	S(9,10) mutagenesis

III. Extraction of Thiocillin Compounds

TclE mutant *B. cereus* starter cultures (5 mL) were grown in LB for 20 hours at 30 °C. Larger cultures (0.5 L LB in 2 L culture baffles culture flasks) were inoculated with 300 µL of starter culture and grown for 68 hours at 30 °C with shaking at 200 rpm. (*tclE* mutant strains were grown in media supplemented with 1µg/mL erythromycin and 25µg/mL lincomycin.) Cultures were harvested and both the cell pellet and spent media were saved. To the pellet, 50

mL methanol was added along with 15 g sodium sulfate. The mixture was vortexed vigorously and allowed to sit for at least 10 minutes. The mixture was then filtered through Whatman filter paper (no. 1) and the methanol was removed by vacuum. Solid was solubilized in 10 mL 33% acetonitrile in water for HPLC analysis. *tclE* mutants that produced compound at low levels were grown in a 5L fermenter in ECPM1 media lacking glycerol (20 g N-Z amine; 3 g Yeast Extract; 1 g KH_2PO_4; 4 g K_2HPO_4; 1 g NH_4Cl; 2.4g K_2SO_4 in 1 L supplemented with 10 mL 100X Trace Elements (5 g EDTA; 0.5 g $FeCl_3$•$6H_2O$; 0.05 g ZnO; 0.01 g $CuCl_2$•$2H_20$; 0.01 g $Co(NO_3)_2$•6H2O; 0.01 g $(NH_4)_6$ Mo_7O_{24} in 1 L) and 2 mL of 500X Mg/Ca solution (203 g $MgCl_2$; 66.2 g $CaCl_2$ in 1 L). Cells and media were harvested after 24 hours and extraction was performed as detailed above, scaled accordingly.

Further purification was accomplished by ethyl acetate extraction. Solvents were removed from the crude compound extracts on a rotary evaporator. The crude residue was then dissolved in 40 mL of 1:1 EtOAc: water. The biphasic solution was transferred to a 60mL separatory funnel, shaken and the organic layer removed. The aqueous layer was washed with a further 20 mL of EtOAc and the combined organics were dried over Na_2SO_4, filtered through a 60 mL coarse fritted glass funnel, and evaporated to dryness. For purposes of assessing the thiocillin content of the individual layers, the residue from the organic layer was redissolved in 10 mL of acetonitrile. 180 µL of the acetonitrile solution was combined with 180 µL of water and 10 µL of this solution was injected into the LC/MS. 10 µL of the aqueous layer was also injected, being careful to avoid the surface organics retained from the extraction. Where compound presence was observed in the LC/MS of this semi-crude isolate, compounds were further purified by preparative RP-HPLC. Compounds were eluted in a gradient of solvents A (0.1% formic acid in water) and B (0.1% formic acid in acetonitrile): 5 min. isocratic 2%B, then increasing to 100%B over 30 min., and finally isocratic at 100%B for 10 min. before returning to 2%B over 5 min. The fraction eluting between 15-25 min. typically contained compounds, which were pooled and used for further LC/MS and MS/MS analysis presented below.

IV. LC-MS and MS/MS Analysis.

High-resolution LC-MS data was collected in positive ion mode, on an Agilent 6520 Accurate-Mass Q-TOF Mass Spectrometer fitted with an electrospray ionization (ESI) source. The capillary voltage was set to 3500 kV, and the fragmentor voltage at 250 V. The drying gas temperature was maintained at 350°C with a flow rate of 12 L/min and a nebulizer pressure of 45 psi. Separation was effected on a Kinetex C18 reverse phase column (2.6µm, 100A, 2.10 x 50 mm, Phenomonex). Compounds were eluted in a gradient of solvents A (0.1% formic acid in water) and B (0.1% formic acid in acetonitrile): 2 min. isocratic 2%B, then increasing to 100%B over 10 min., and finally isocratic at 100%B for 2 min. before returning to 2%B over 1 min. As described above, at least two analytical runs were performed for extracts from each mutant: crude extract was used in the first run in order to better search for the presence of trace quantities of all tailored states and subsequently semi-purified compounds (from preparative HPLC) were examined in a second run to obtain high resolution masses with lower ppm error than those observed in the crude runs. Extracted ion chromatograms are illustrated below. For LC/MS figures, overlayed extracted ion chromatograms were overlayed and colored by compound to produce the top chromatogram. MS for each compound is listed below. In selected cases, exemplified by Cmpd 1 in LC/MS fig 2, the co-elution of two compounds differing in mass by 2 m/z appears to change the isotopic distribution. This is an artifact of co-elution of compounds and does not affect the accuracy of the primary isotopic peak.

Additional structural analysis was accomplished by targeted CID-MS/MS. For all samples examined, the collision energy was ramped from 40 to 55 eV. Composite/overlay spectra for isolates from the C9S and S(9,10) mutant strains are illustrated below together with a scheme of the observed peptide bond fragmentation pathway. Both raw spectra and a regraph are

displayed. The regraph is comprised of all peaks from the raw, normalized to percent peak abundances, and filtered for a peak abundance greater than 2:1 signal to noise ratio. Peaks in the overlays have been color coded to indicate whether they are ions specific to and therefore characteristic of the smaller or larger ring resulting from the mutant or else ions common to both ring sizes. In addition to peptide bond fragmentations, many of the observed fragments can be assigned to pathways involving single electron ionization or cission of the thiazole ring in accord with the available analytical literature on thiazoles.[4] Several of these sub-fragmentation products were confirmed by MS^3 (data not shown). All assigned peaks are listed in the accompanying tables.

---

[1] Sambrook, J.; Fitsch, E. F.; Maniatis, T. *Molecular Cloning. A Laboratory Manual. 3rd ed*; Cold Spring Harbor Laboratory Press: Cold Spring Harbor, NY, 2001.

[2] Acker, M. G.; Bowers, A. A.; Walsh, C. T. *J. Am. Chem. Soc.* **2009**, *131*, 17563-17565

[3] Brown, L. C.; Acker, M. G.; Clardy, J.; Walsh, C. T.; Fischbach, M. A. *Proc Natl Acad Sci U S A* **2009**, *106*, 2549-53

[4] (a) Ketterning, J.; Colombo, L.; Ferrari, P.; Tavecchia, P.; Nebuloni, M.; Vekey, K.; Gallo, G.; Selva, E., *J. Antibiotics* **1991**, *44*, 702-15 (b) Kurz, M.; Sottani, C.; Bonfichi, R.; Lociuro, S.; Selva, E., *J. Antibiotics* **1994**, *47*, 1564-7 (c) Ferrari, P.; Colombo, L.; Stella, S.; Selva, E.; Zaerilli, L. F., *J. Antibiotics* **1995**, *48*, 1304-11 (e) McGibbon, G. A.; Hrusak, J.; Lavorato, D. J.; Schwarz, H.; Terlouw, J. K., *Chem. Eur. J.* **1997**, *3*, 232-6 and references therein.

V. LC-MS Traces and Extracted Ion Chromatograms for Isolated Mutant Compounds

LC/MS Figure 1: Extracts from Δ*T3* cultures.

Compound	R^1, R^2, R^3 (additional)	Color	RT	Expected $(M+H)^+$	Observed $(M+H)^+$	Error (ppm)	Expected $(M+Na)^+$	Observed $(M+Na)^+$	Error (ppm)
1	H, CH3, red (+H2O, + succ. GA)	Black	8.984	1338.3076	1338.3044	2.39	1360.2896	1360.2853	3.16
2	H, CH3, red (+H2O, + succ. A)	Red	9.067	1281.2861	1281.2825	2.81	1303.2681	1303.267	0.84
3	H, H, red (-H2O)	Dark Green	9.586	1043.1696	1043.1667	2.78	1065.1516	1065.1564	-4.51
4	H, CH3, red (+2xH2O,H2)	Navy Blue	9.728	1095.2221	1095.2213	0.73	1117.2041	1117.2025	1.43
5	H, CH3, red (-H2O)	Purple	10.177	1057.1853	1057.1836	1.61	1079.1673	1079.1653	1.85
6	H, CH3, ox (-H2O)	Brown	10.437	1055.1696	1055.1672	2.27	1077.1516	1077.1507	0.84

23-member ΔT3 structures

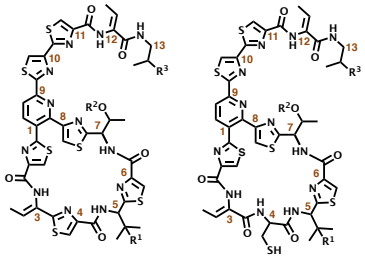

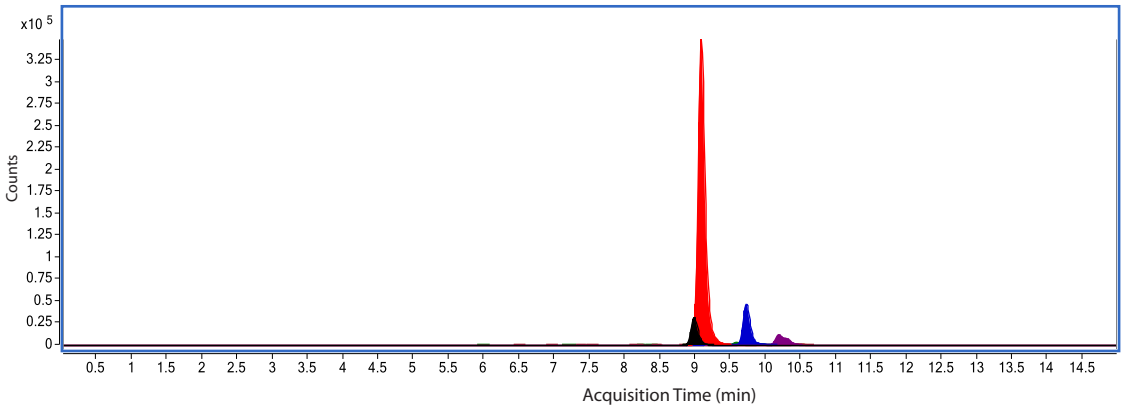

Linear ΔT3 structures

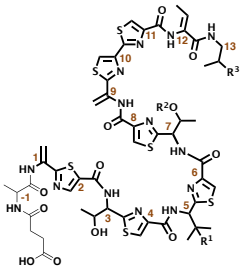

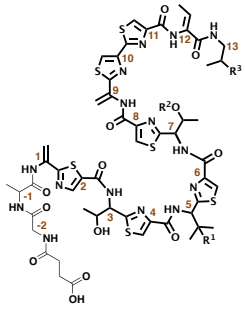

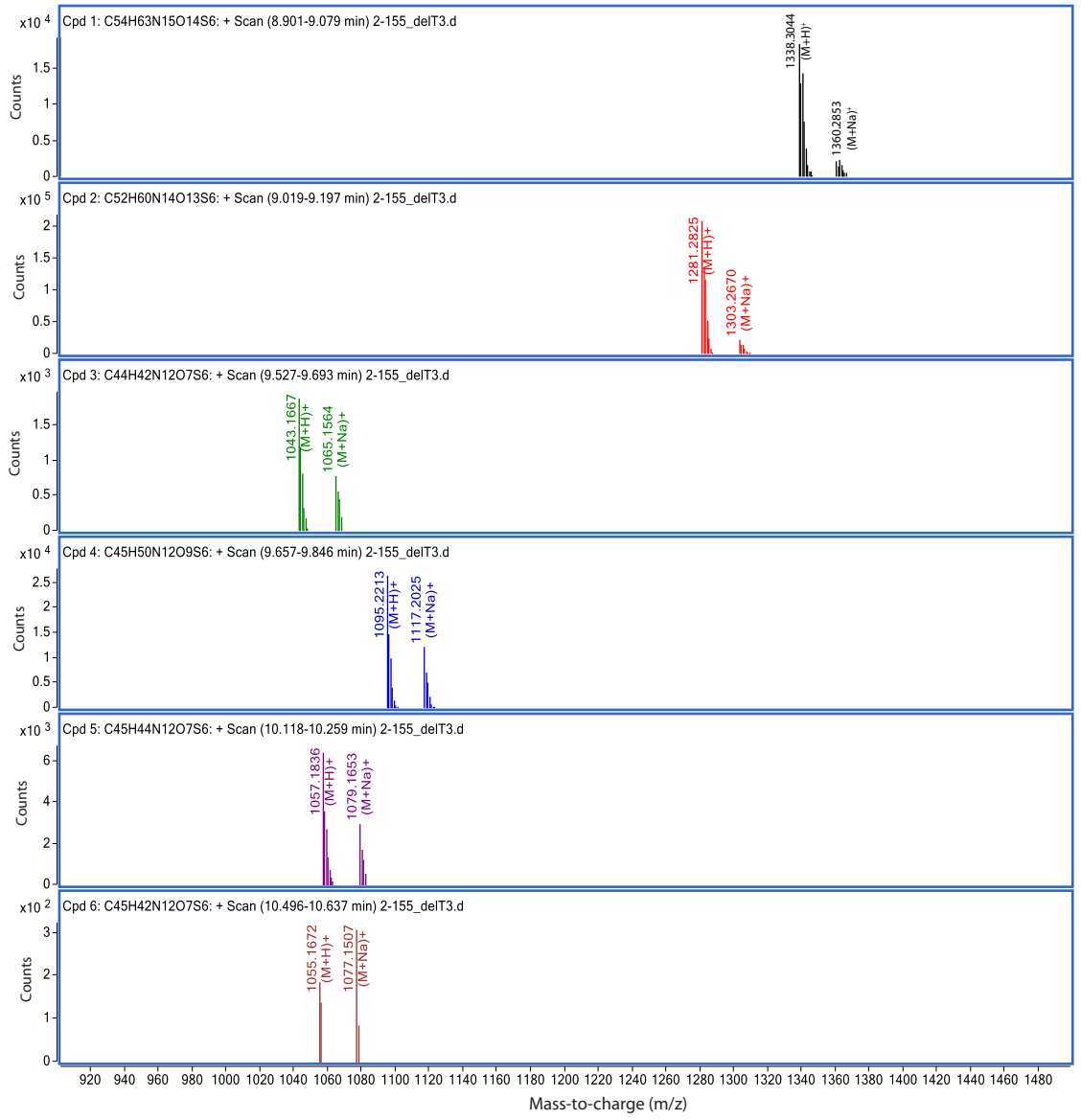

LC/MS Figure 2: Extracts from *G(3,4)* cultures.

Compound	R^1, R^2, R^3	Color	RT	Expected $(M+H)^+$	Observed $(M+H)^+$	Error (ppm)	Expected $(M+Na)^+$	Observed $(M+Na)^+$	Error (ppm)
1	OH, H, red (-1xH2O)	Black	8.981	1199.2231	1199.2225	0.50	1221.205	1221.2056	-0.49
2	H, H, red (-1xH2O)	Red	8.819	1201.2388	1201.2277	9.24	1223.2207	1223.2165	3.43
3	OH, CH3, red (-1xH2O)	Dark Green	8.836	1231.2493	1231.2498	-0.41	1253.2312	1253.2292	1.60
4	OH, H, red (-2xH2O)	Navy Blue	9.821	1217.2337	1217.2304	2.71	1239.2156	1239.2133	1.86
5	H, CH3, red	Purple	9.272	1233.265	1233.2593	4.62	1255.2469	1255.2544	-5.97
6	OH, CH3, red (-2xH2O)	Brown	9.465	1213.2388	1213.2383	0.41	1235.2207	1235.2206	0.08
7	H, CH3, red (-1xH2O)	Lime Green	9.272	1215.2544	1215.2535	0.74	1237.236	1237.2374	-1.13

29-member G(3,4) structures

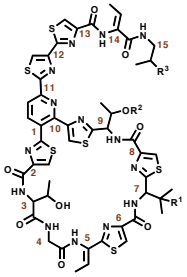

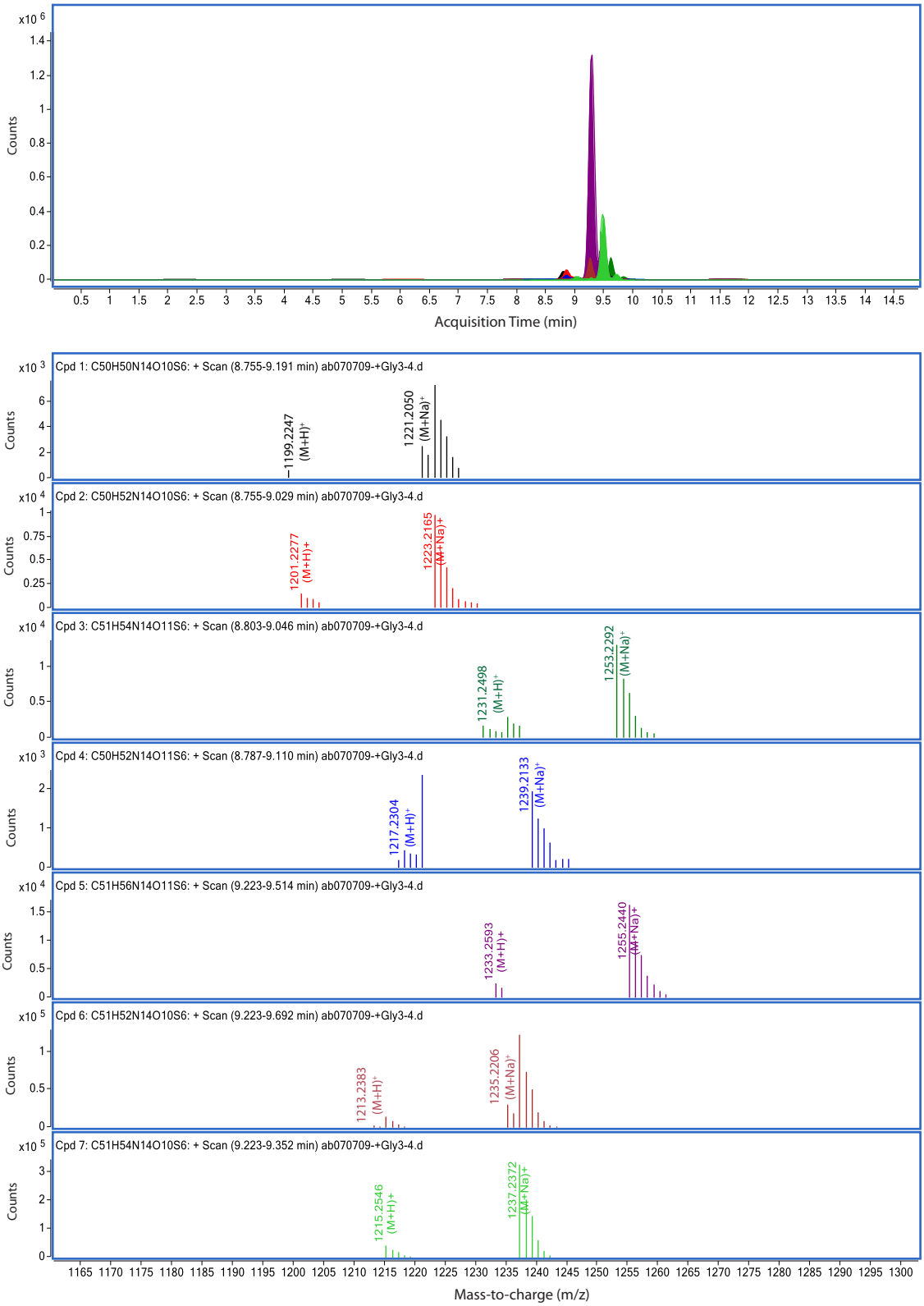

LC/MS Figure 3: Extracts from *GG(3,4)* cultures.

Compound	R^1, R^2, R^3	Color	RT	Expected $(M+H)^+$	Observed $(M+H)^+$	Error (ppm)	Expected $(M+Na)^+$	Observed $(M+Na)^+$	Error (ppm)
1	OH, CH3, red (-2xH2O)	Red	6.731	1288.2708	1288.2704	0.31	1310.2527	1310.2541	-1.07
2	H, CH3, ox (-1xH2O)	Dark Green	7.668	1270.2602	1270.258	1.73	1292.2421	1292.2412	0.70
3	H, CH3, red (-1xH2O)	Navy Blue	7.571	1272.2759	1272.276	-0.08	1294.2578	1294.2581	-0.23
4	H, CH3, ox (-2xH2O)	Purple	7.845	1252.2497	1252.2488	0.72	1274.2316	N/A	N/A
5	H, CH3, red (-2xH2O)	Brown	7.732	1254.2653	1254.2662	-0.72	1276.2472	1276.248	-0.63

32-member GG(3,4) structures

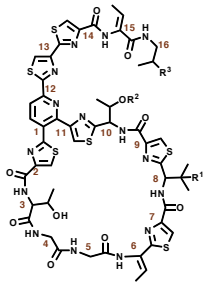

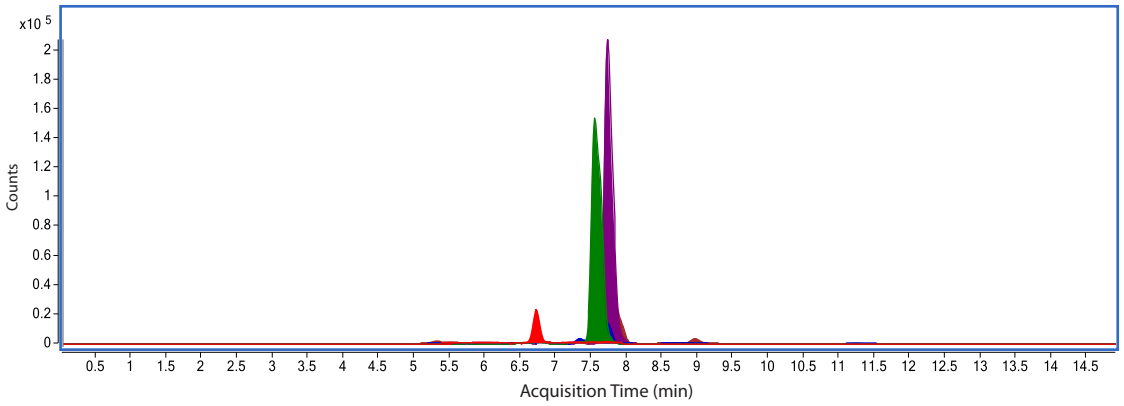

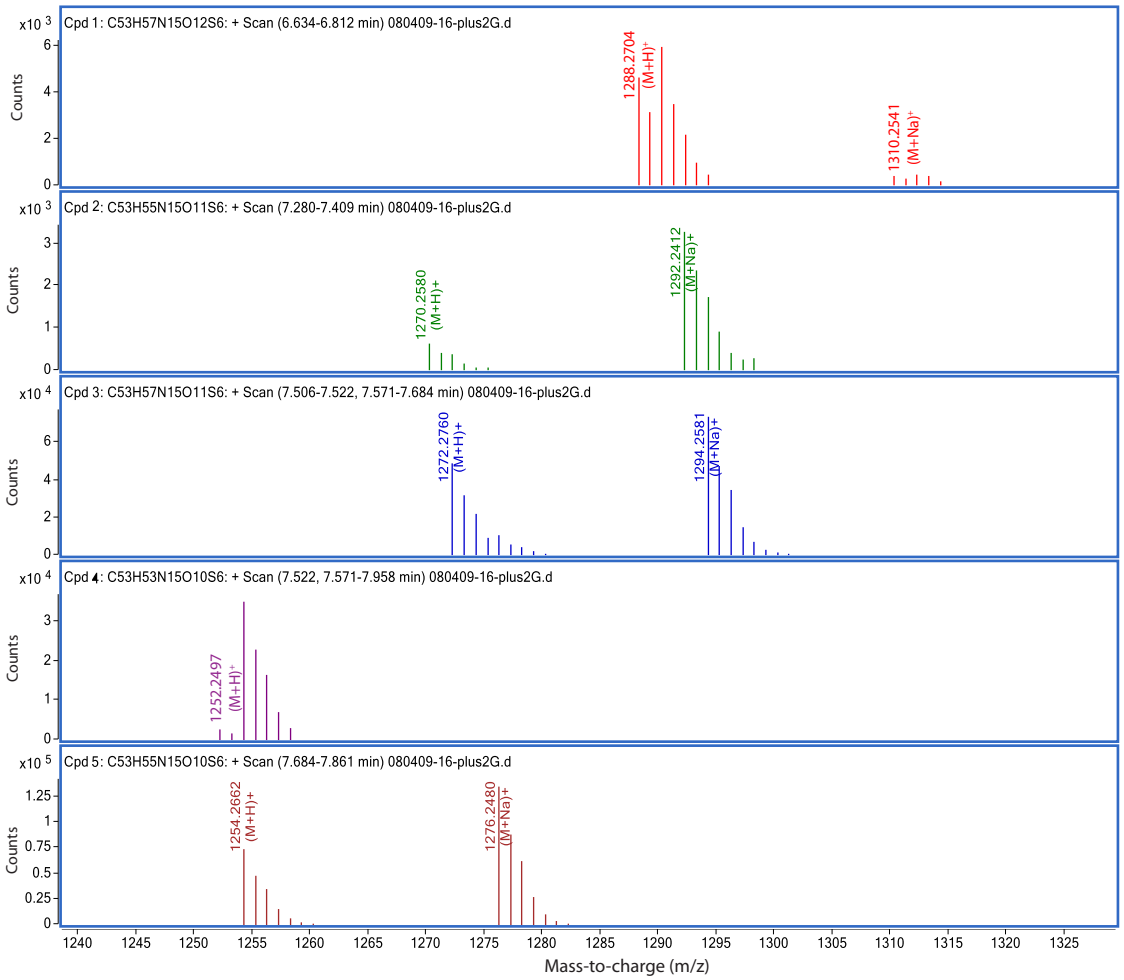

LC/MS Figure 4: Extracts from *GGG(3,4)* cultures.

Compound	R^1, R^2, R^3	Color	RT	Expected $(M+H)^+$	Observed $(M+H)^+$	Error (ppm)	Expected $(M+Na)^+$	Observed $(M+Na)^+$	Error (ppm)
1	H, CH3, red (-1xH2O)	Black	7.476	1329.2974	1329.3008	3.21	1351.2793	1351.2835	3.21
2	H, CH3, red (-2xH2O)	Red	7.522	1311.2868	1311.2897	-2.21	1333.276	N/A	N/A

35-member GGG(3,4) structures

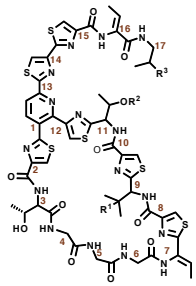

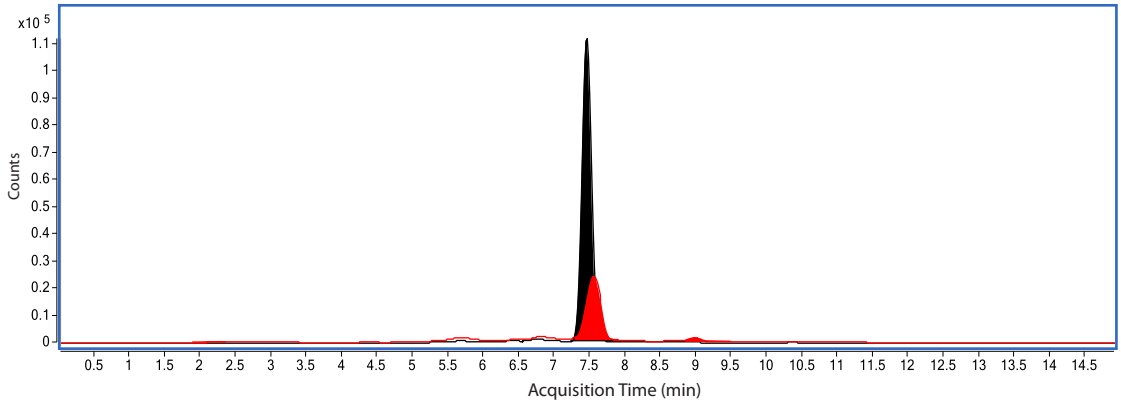

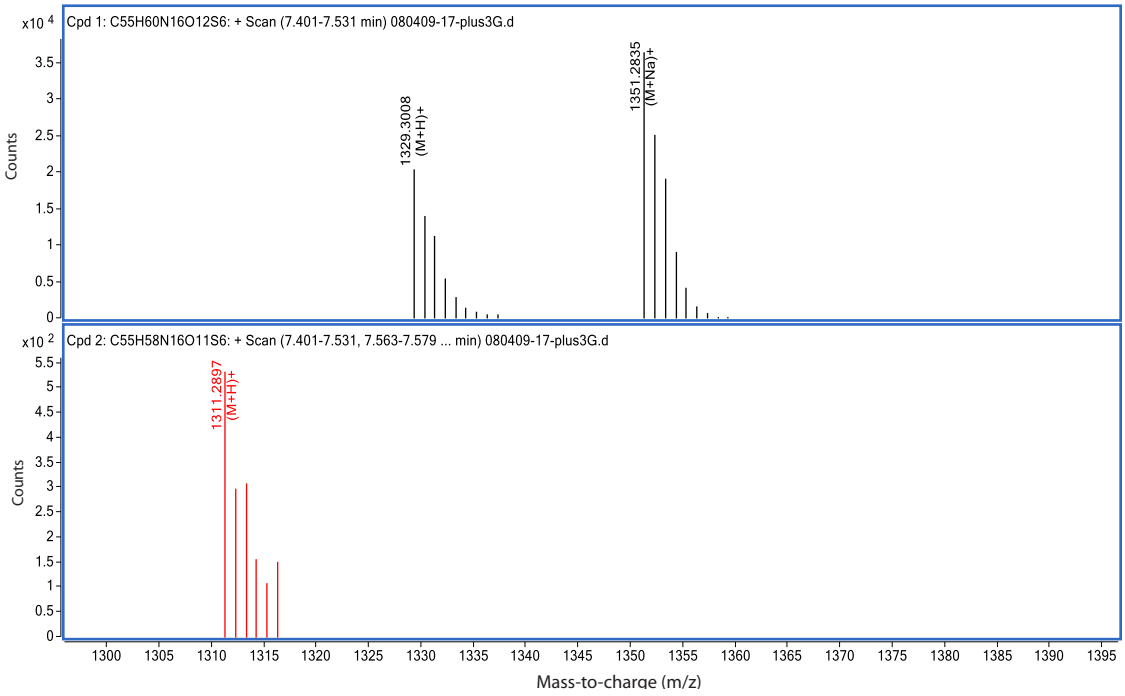

LC/MS Figure 5: Extracts from *S(1,2)* cultures.

Compound	R^1, R^2, R^3	Color	RT	Expected $(M+H)^+$	Observed $(M+H)^+$	Error (ppm)	Expected $(M+Na)^+$	Observed $(M+Na)^+$	Error (ppm)
1	OH, CH3, red (wild type)	Black	8.833	1174.2279	1174.2256	1.96	1196.2098	N/A	N/A
2	OH, CH3, ox (wild type)	Red	9.01	1172.2122	1172.2136	-1.19	1194.1941	N/A	N/A
3	H, CH3, red (-1xH2O)	Dark Green	9.268	1227.2551	1227.2531	1.63	1249.2370	1249.2375	-0.40
4	H, CH3, ox (-1xH2O)	Navy Blue	9.429	1225.2395	1225.2374	1.71	1247.2214	1247.2246	-2.57

26-member S(1,2) structures

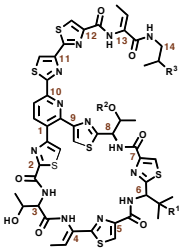

29-member S(1,2) structures

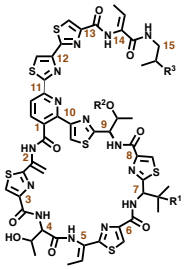

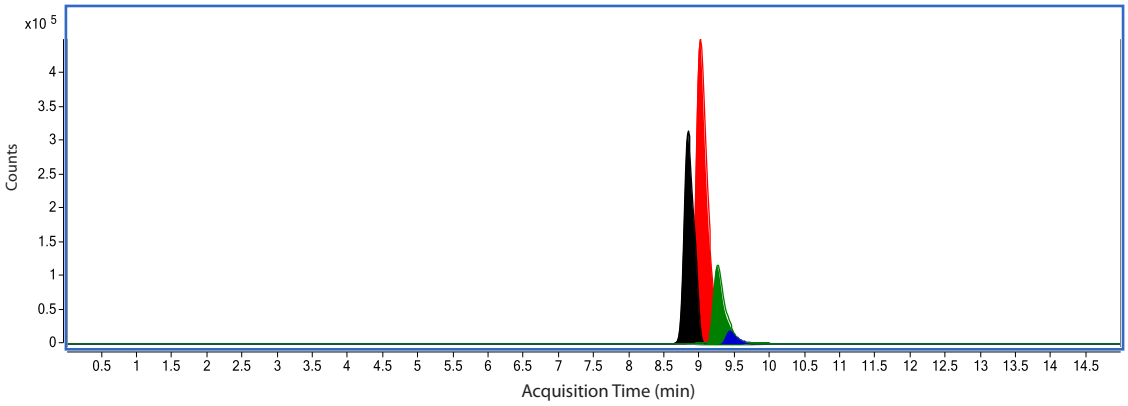

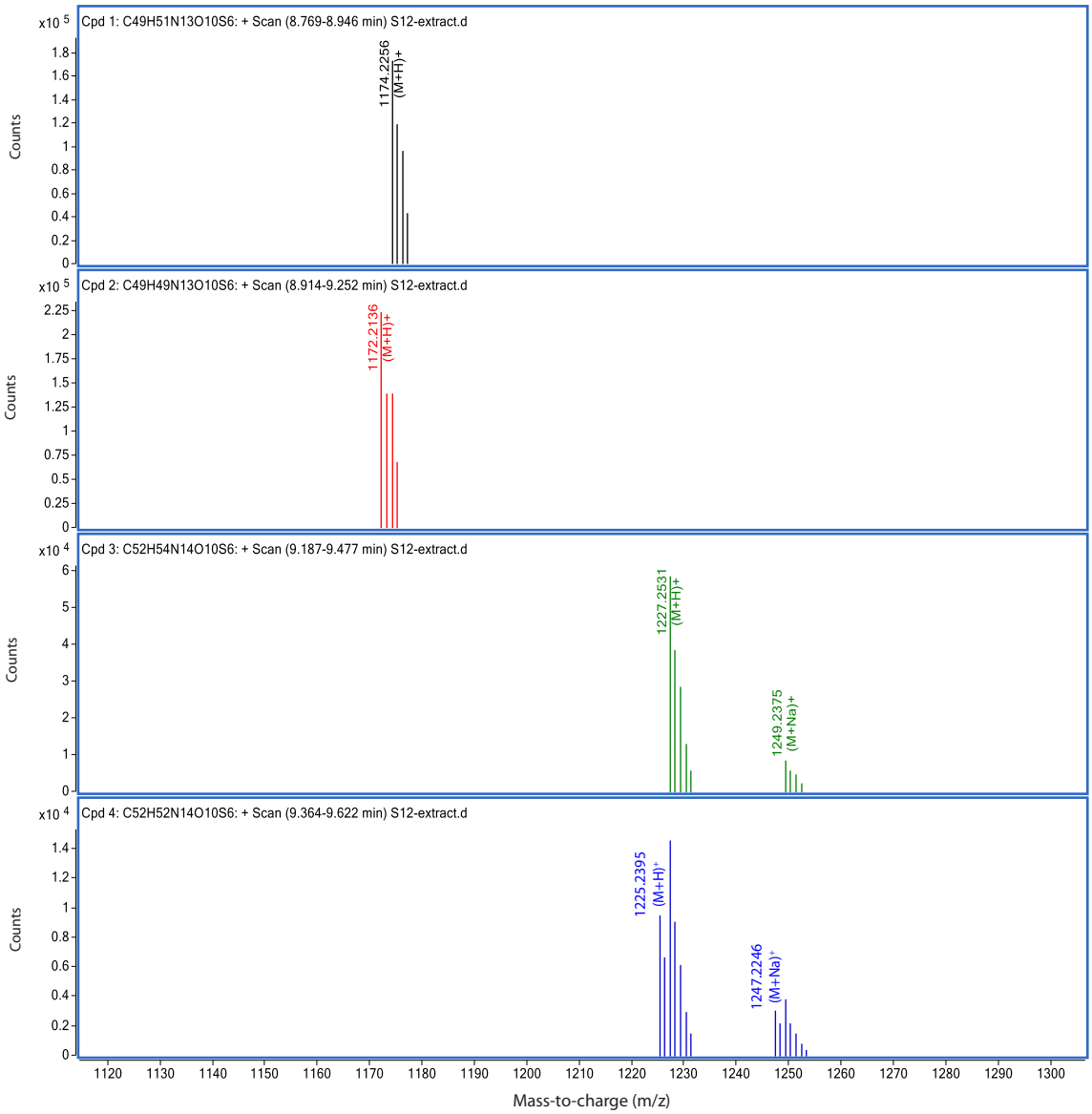

LC/MS Figure 6: Extracts from *C2S* cultures.

Compound	R^1, R^2, R^3	Color	RT	Expected $(M+H)^+$	Observed $(M+H)^+$	Error (ppm)	Expected $(M+Na)^+$	Observed $(M+Na)^+$	Error (ppm)
1	H, CH3, red (alcohol)	Black	8.628	1162.2820	1162.2809	0.95	1184.2646	N/A	N/A
2	OH, CH3, red (-1xH2O)	Red	8.756	1160.2664	1160.2645	1.64	1182.2489	N/A	N/A
3	H, CH3, red (-1xH2O)	Dark Green	8.789	1142.2558	1142.2559	-0.09	1164.2383	N/A	N/A
4	H, CH3, ox (-1xH2O)	Navy Blue	8.95	1144.2715	1144.2706	0.79	1166.2540	1166.2577	-3.17

C2S alcohol structure

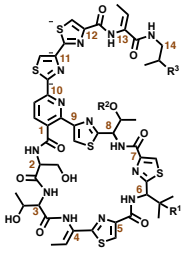

C2S oxazoline structure

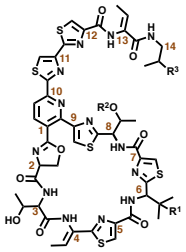

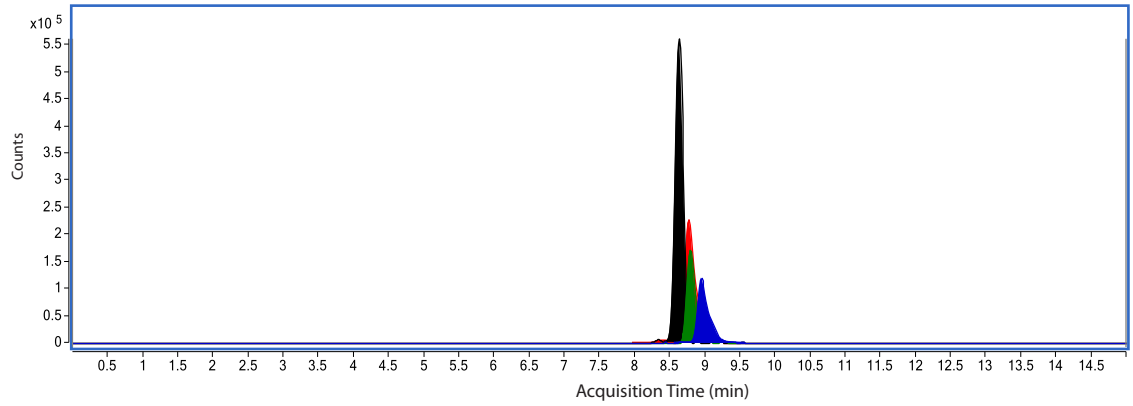

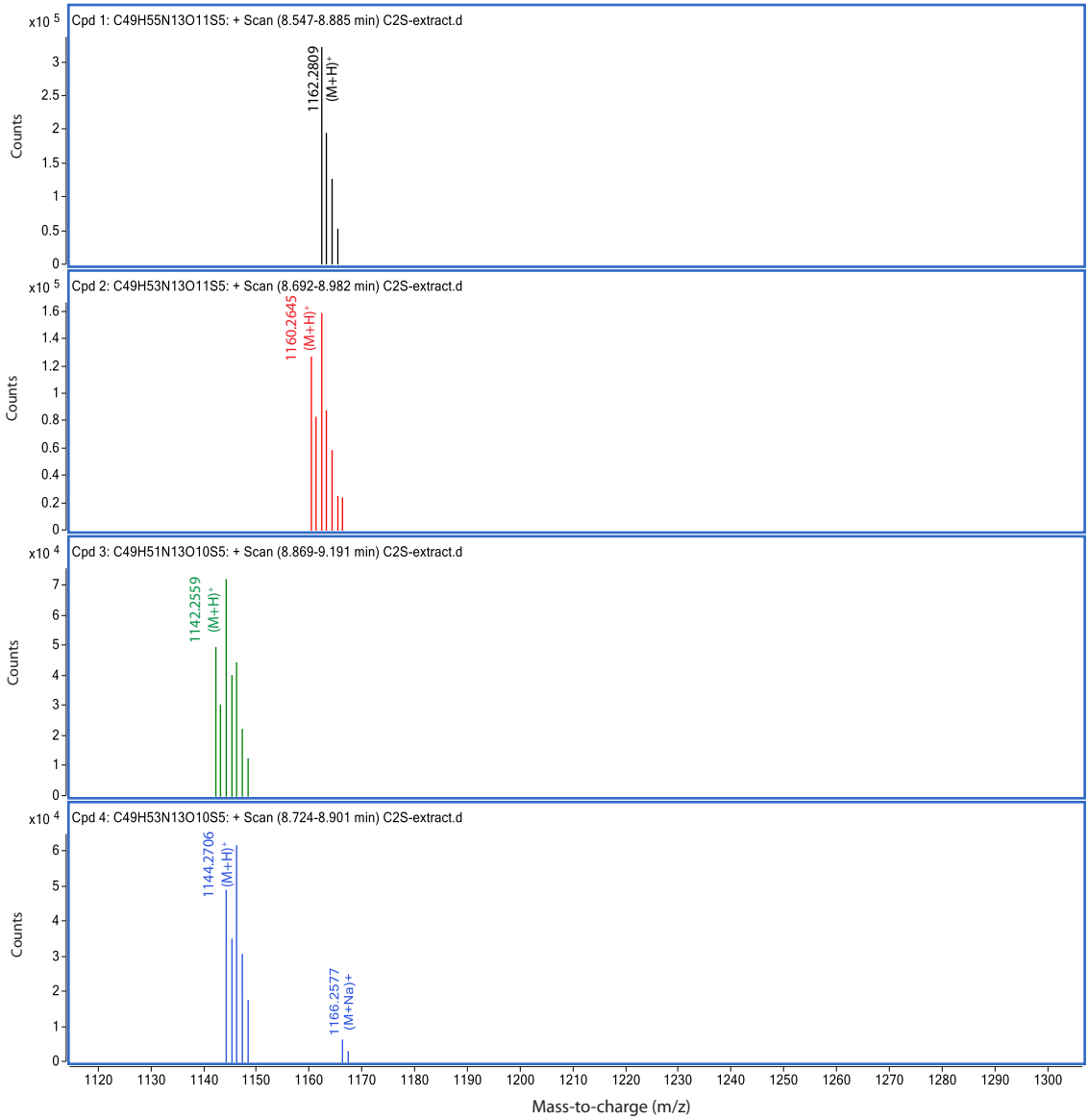

LC/MS Figure 7: Extracts from *C9S* cultures.

Compound	R^1, R^2, R^3 (R^4)	Color	RT1	RT2	Expected $(M+H)^+$	Observed $(M+H)^+$	Error (ppm)	Expected $(M+Na)^+$	Observed $(M+Na)^+$	Error (ppm)
1	H, H, red (alcohol)	Black	7.284	8.807	1148.2670	1148.2588	7.14	1170.2489	N/A	N/A
2	OH, H, red (-1xH2O)	Red	7.308	8.784	1146.2514	1146.2432	7.15	1168.2333	N/A	N/A
3	H, H, red (-1xH2O)	Dark Green	7.367	9.173	1130.2564	1130.2475	7.87	1152.2383	1152.2419	-3.12
4	H, H, ox (-1xH2O)	Navy Blue	7.402	9.339	1128.2408	1128.2358	4.43	1150.2227	1150.2169	5.04

23-member C9S structures

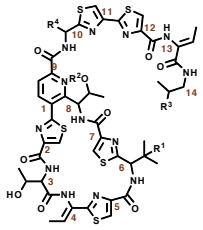

26-member C9S structures

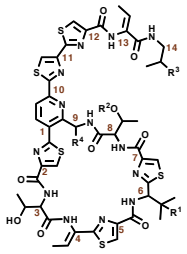

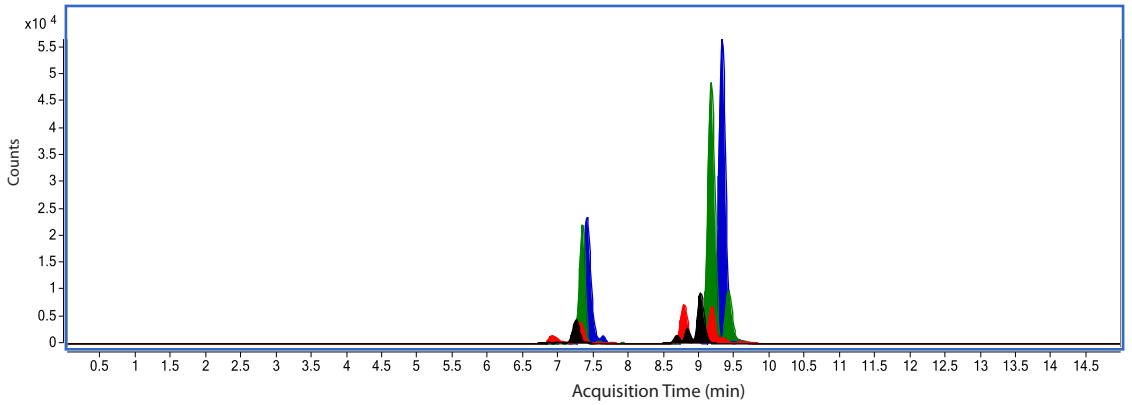

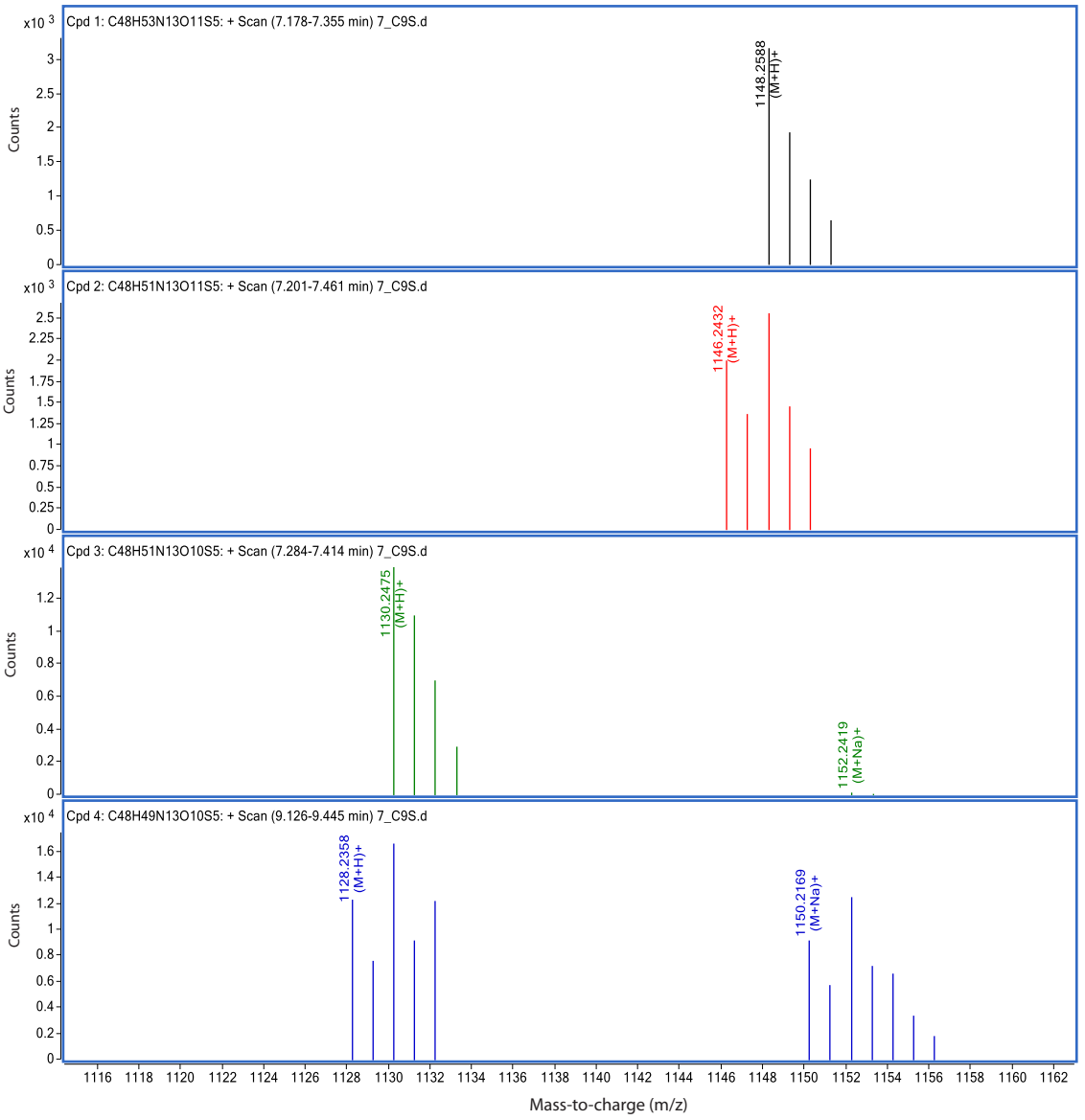

LC/MS Figure 8: Extracts from *S(9,10)* cultures.

Compound	R^1, R^2, R^3	Color	RT1	RT2	Expected $(M+H)^+$	Observed $(M+H)^+$	Error (ppm)	Expected $(M+Na)^+$	Observed $(M+Na)^+$	Error (ppm)
1	H, H, red (-1xH2O)	Black	7.651	9.4860	1213.2395	1213.2314	6.68	1235.2214	1235.2180	2.75
2	H, H, ox (-1xH2O)	Red	7.667	9.1320	1211.2238	1211.2209	2.39	1233.2057	1233.2036	1.70
3	OH, H, red (-1xH2O)	Dark Green	9.1	N/A	1229.2344	1229.2289	4.47	1251.2163	N/A	N/A

26-member S(9,10) structures

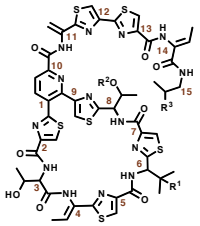

29-member S(9,10) structures

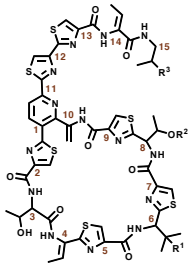

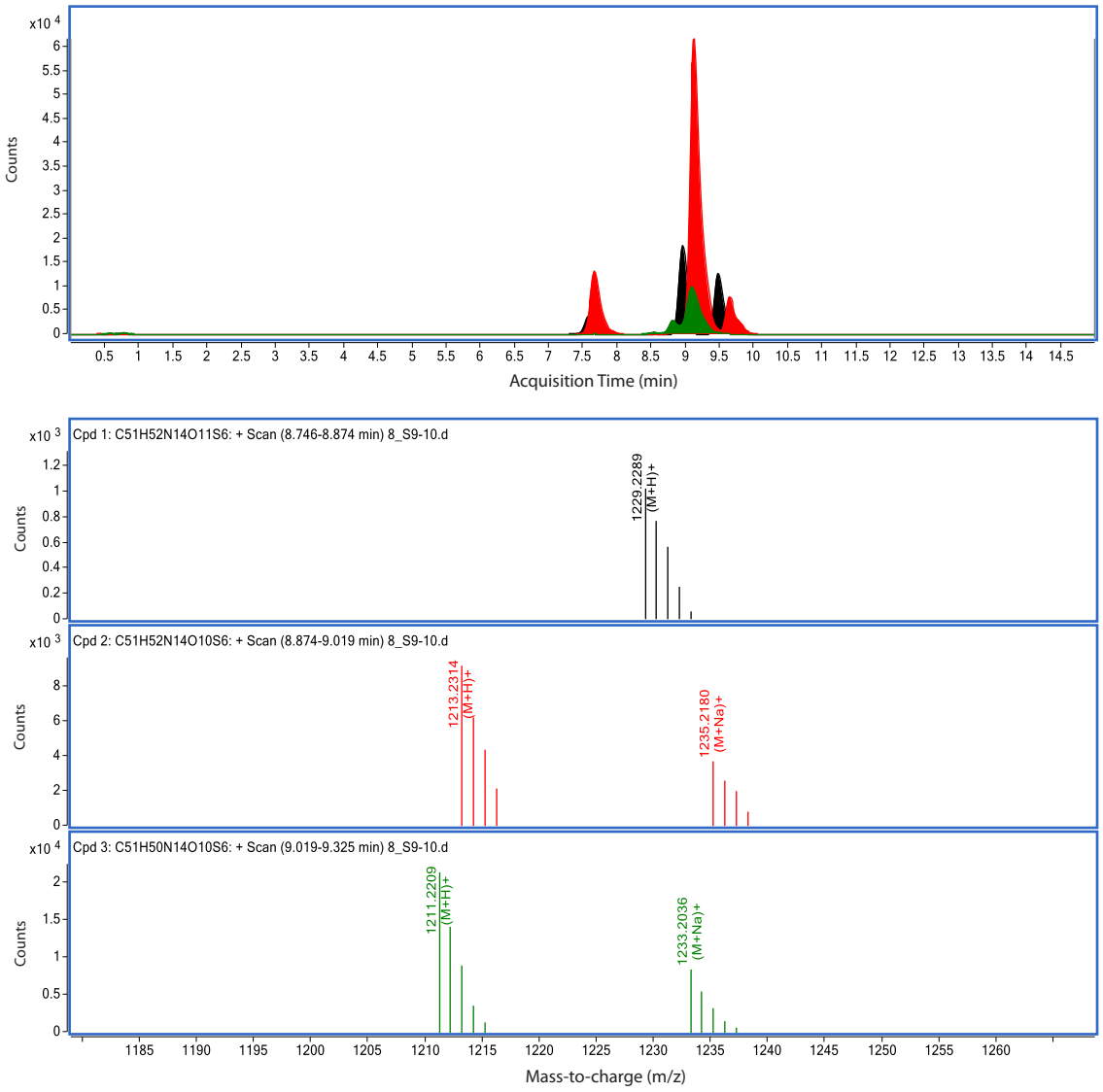

VI. MS/MS Fragmentation Data and Ion Assignments

MS/MS Figure 1: Significant fragments from a Δ*T3* compound.

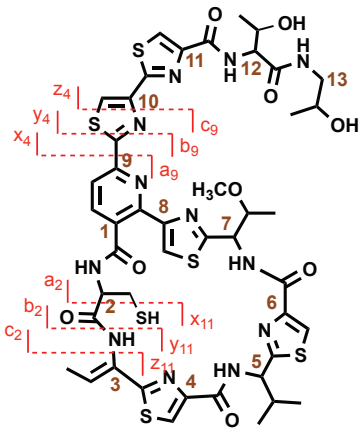

23-membered ring product
parent ion = 1095.2221

ΔT3 ms/ms data summary				
Observed	Predicted	Diff (ppm)	Abund%	Ion
1077.2059	1077.2115	-5.2	6.23	M-H2O
1045.1882	1045.1853	2.8	7.47	M-H2O-CH3OH
1027.1608	1027.1747	-13.5	9.52	M-2H2O-CH3OH
988.1285	988.1274	1.1	26.37	b12-CH3OH
970.1078	970.1169	-9.4	17.27	b12-CH3OH-H2O
905.0780	905.0903	-13.6	5.16	b11-CH3OH
702.1271	702.1291	-2.8	8.85	a2-c6
684.1144	684.1186	-6.1	14.74	a2-c6-H2O
670.0996	670.1029	-4.9	67.35	a2-c6-CH3OH
652.0886	652.0924	-5.8	57.2	a2-c6-CH3OH-H2O
350.0622	350.0628	-1.7	10.14	z11-y7
184.0414	184.0539	-67.9	19.07	y11-z9-H2O
167.0291	167.0274	10.2	35.89	y11-y9-H2O

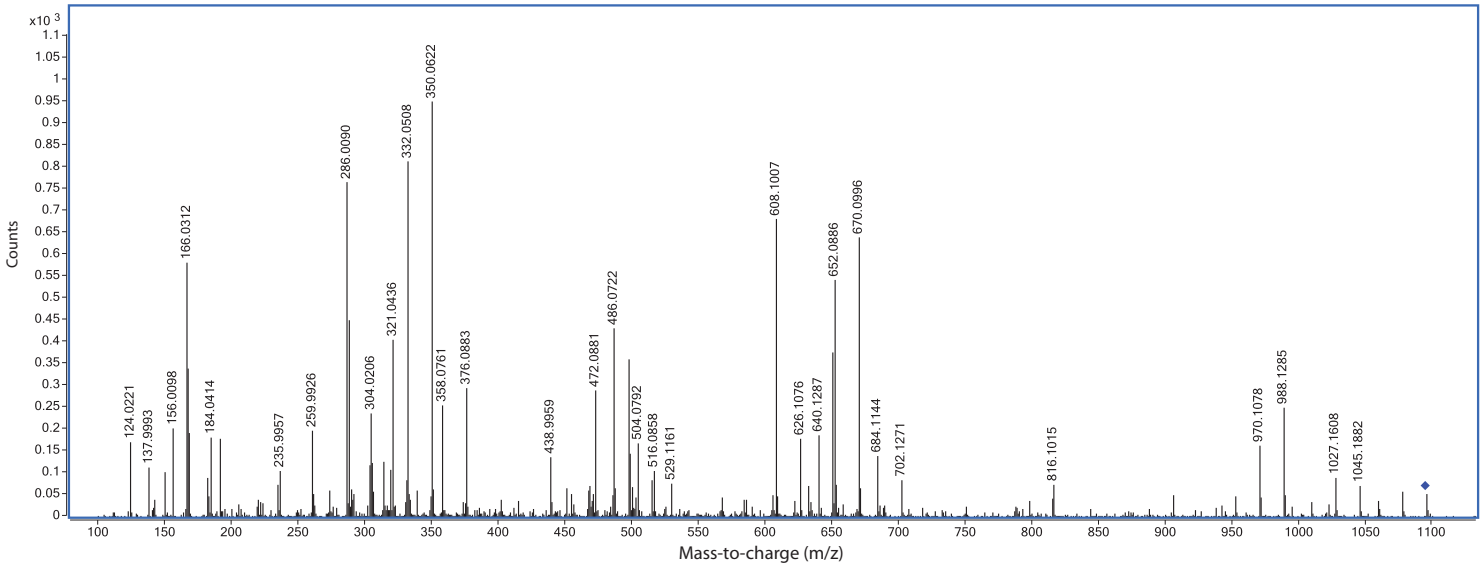

MS/MS Figure 2: MS/MS spectra of *G(3,4), GG(3,4), and GGG(3,4)* compounds.

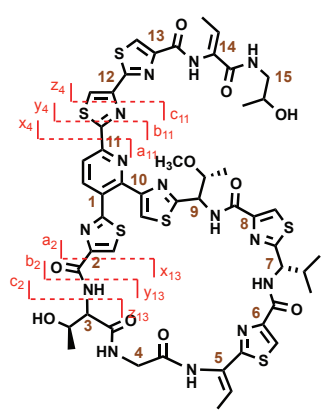

29-membered ring product
parent ion = 1215.2544

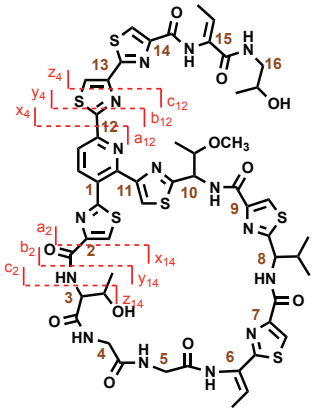

32-membered ring product
parent ion = 1272.2759

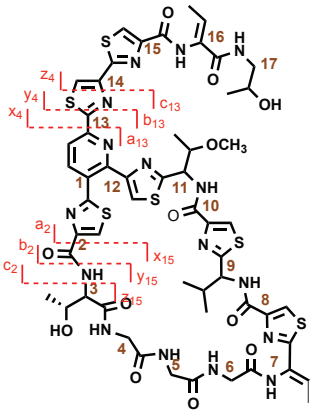

35-membered ring product
parent ion = 1329.2974

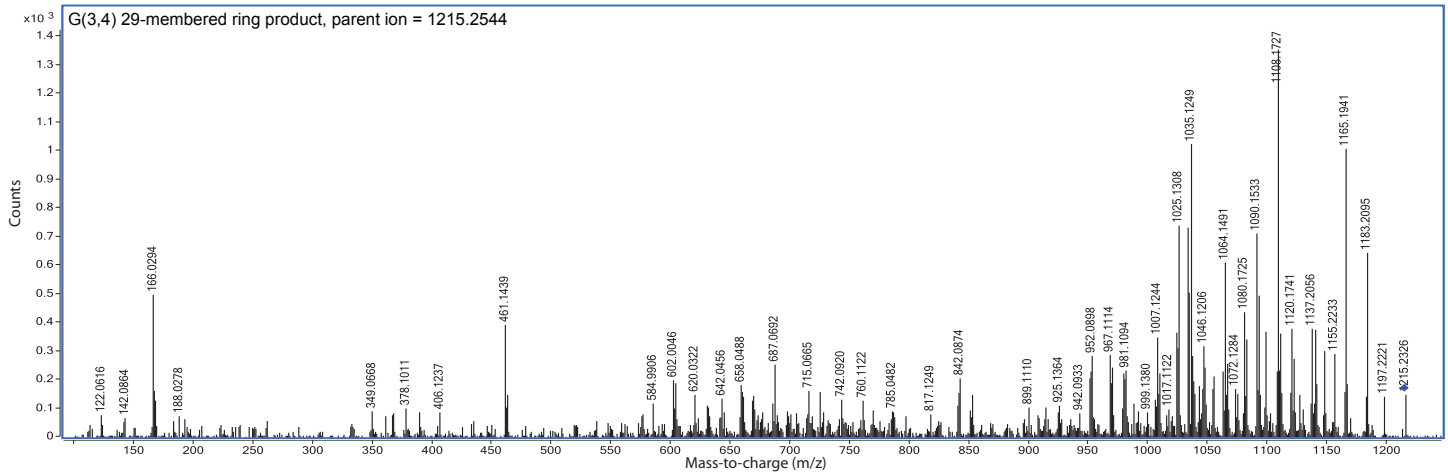

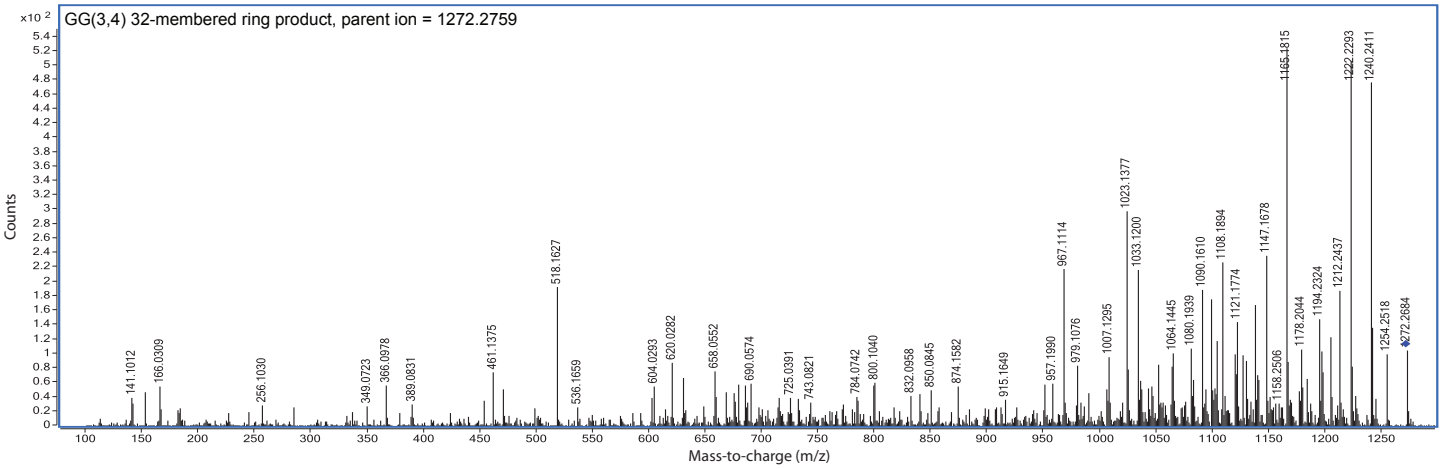

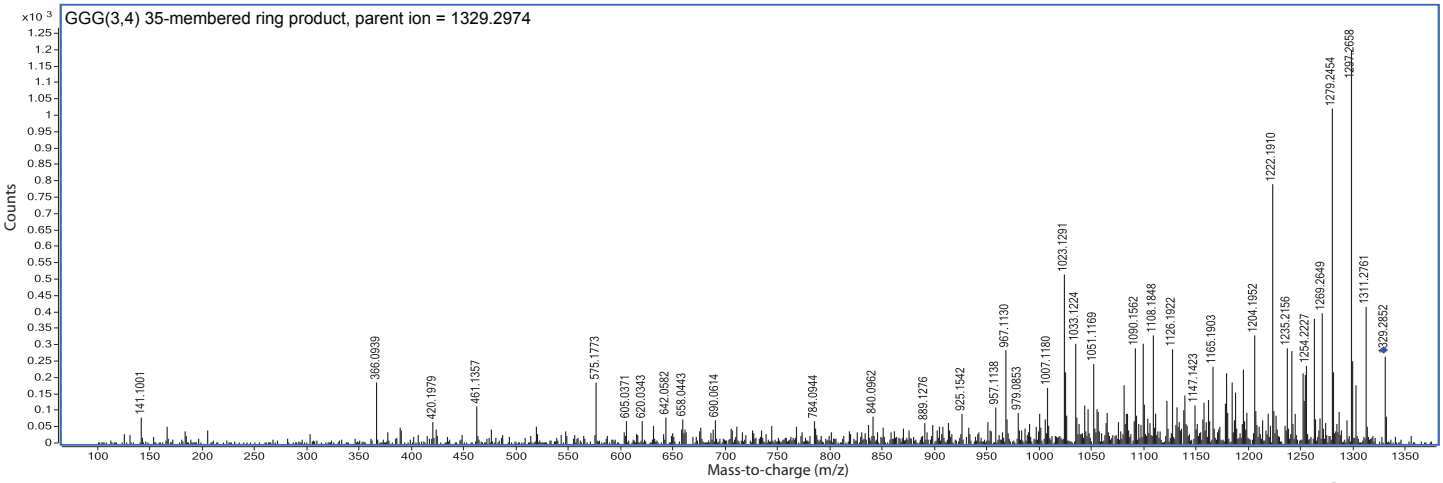

MS/MS Figure 2 (continued): Significant fragments from *G(3,4), GG(3,4), and GGG(3,4)* compounds.

The most distinctive fragmentation pathway in the glycine incorporation mutants involved loss of the glycine residues. As a result, all three mutants, *G(3,4),* *GG(3,4),* and *GGG(3,4)* exhibited a common core subset of ions. Additionally, there were ions common to *GG(3,4),* and *GGG(3,4),* but not *G(3,4),* due to the ability of both of these compounds to fragment in ways that left two glycine residues remaining. This subset of common and unique ions was employed predominantly to confirm the identification of the isolated compounds. They are listed in the table below using notation for the structure of GGG(3,4).

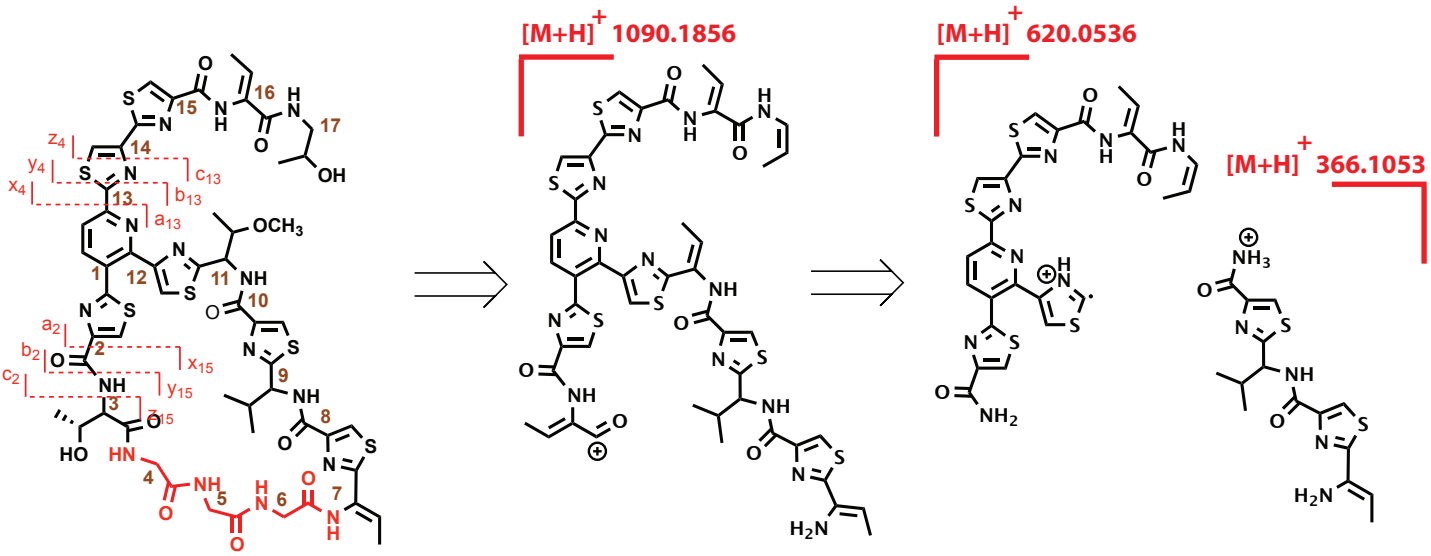

G, GG, and GGG (3,4) insertion ms/ms data summary										
Expected	Observed G(3,4)	Diff (ppm)	Abund%	Observed GG(3,4)	Diff (ppm)	Abund%	Observed GGG(3,4)	Diff (ppm)	Abund%	Ion*
1311.2868	--	--	--	--	--	--	1311.2761	8.2	18.46	M-H2O
1279.2606	--	--	--	--	--	--	1279.2454	11.9	100	M-H2O-CH3OH
1254.2653	--	--	--	1254.2518	10.8	19.1	1254.2227	34.0	9.58	c3-a4-H2O
1222.2391	--	--	--	1222.2293	8.0	96.43	1222.1910	39.4	72.57	c3-a4-H2O-CH3OH
1165.2177	1165.1941	20.3	57.26	1165.1815	31.1	100	1165.1817	30.9	22.05	M-H2O-CH3OH
1108.1962	1108.1727	21.2	100	1108.1894	6.1	43.46	1108.1932	2.7	32.61	b3-b4-H2O-CH3OH
1090.1856	1090.1533	29.6	26.12	1090.1610	22.6	32.2	1090.1620	21.6	12.36	b3-b4-2H2O-CH3OH
1023.1183	1023.1355	-16.8	15.78	1023.1377	-19.0	56.97	1023.1392	-20.4	30.91	c3-b4-z1-2H2O
967.1172	967.1114	6.0	7.6	967.1114	6.0	41.59	967.1155	1.8	19.21	b3-b4-z2-2H2O
620.0536	620.0322	34.5	7.2	620.0282	41.0	16.89	620.0301	37.9	5.43	c2-a9-H2O
366.1053	366.0978	20.5	5.34	366.0978	20.5	10.89	366.0997	15.3	7.21	y13-z9
141.1022	141.1024	-1.4	5.92	141.1012	7.1	7.47	141.0954	48.2	8.16	y2-H2O

*Ion labeling based on GGG(3,4) numbering system

MS/MS Figure 3: Fragmentation of compounds from *C9S* cultures.

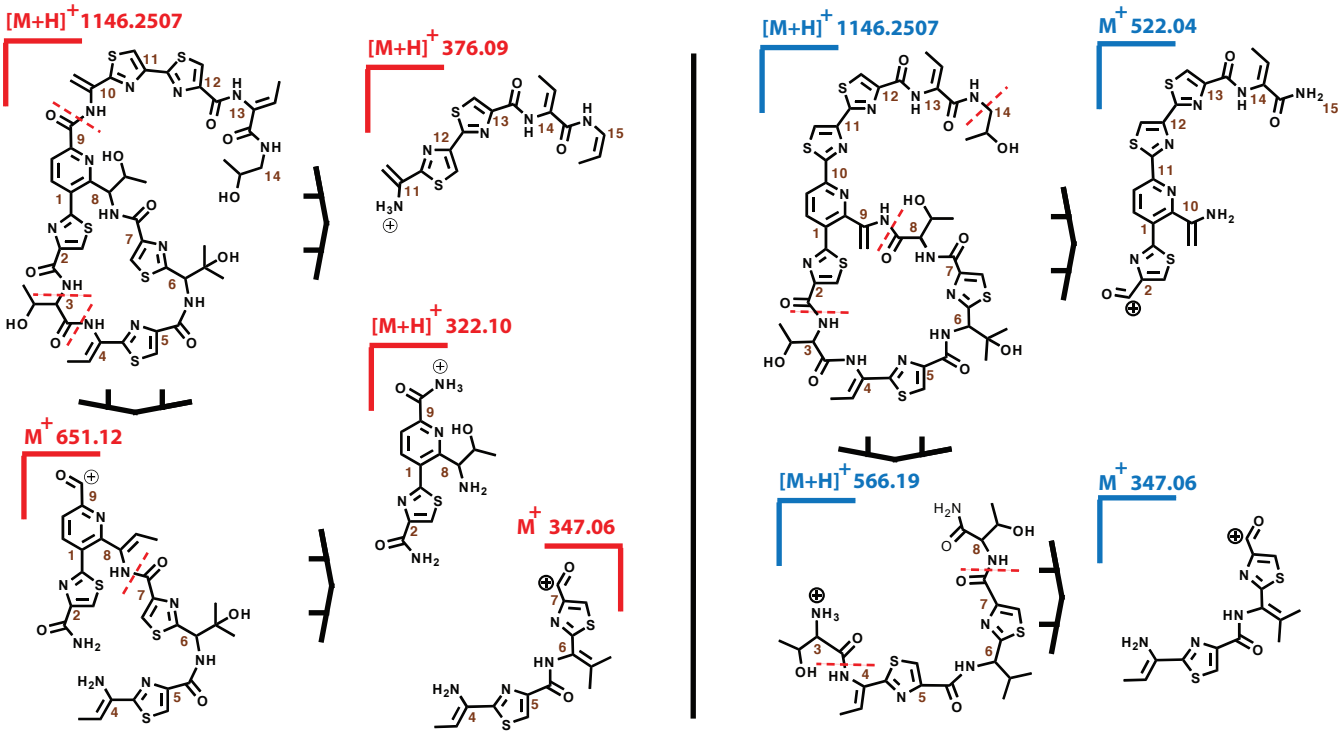

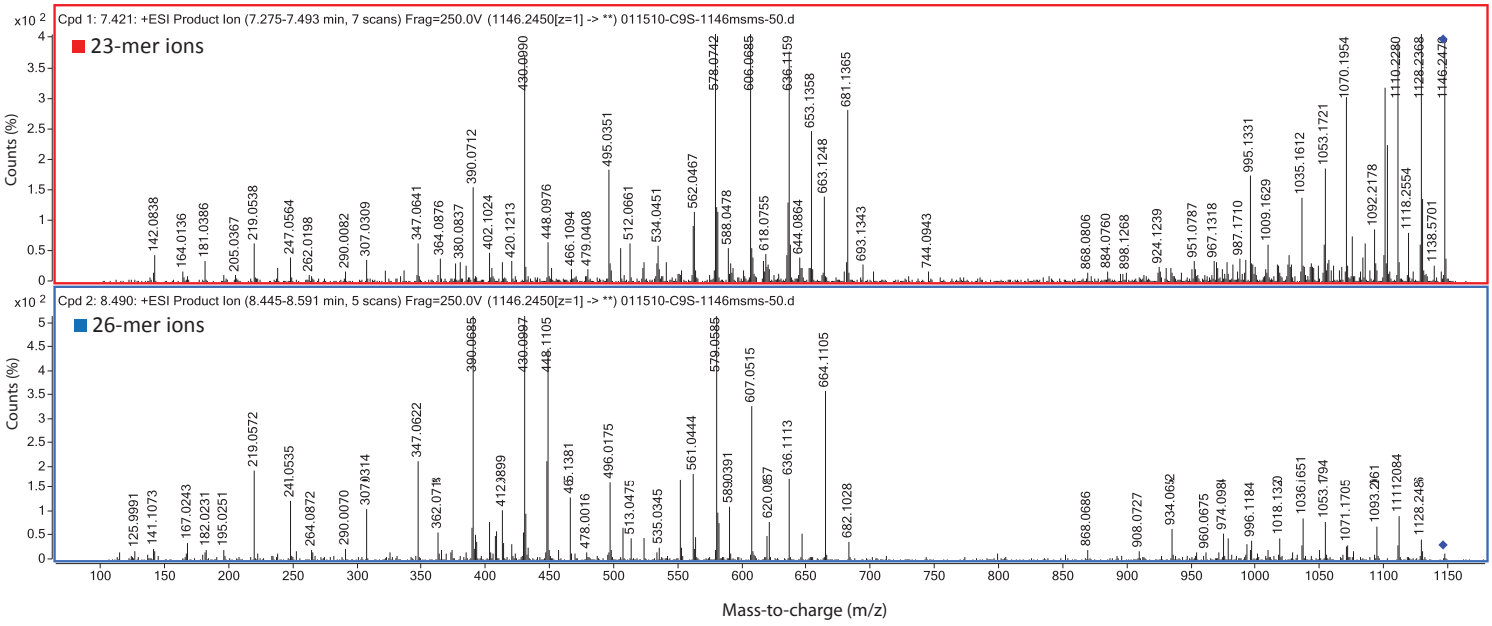

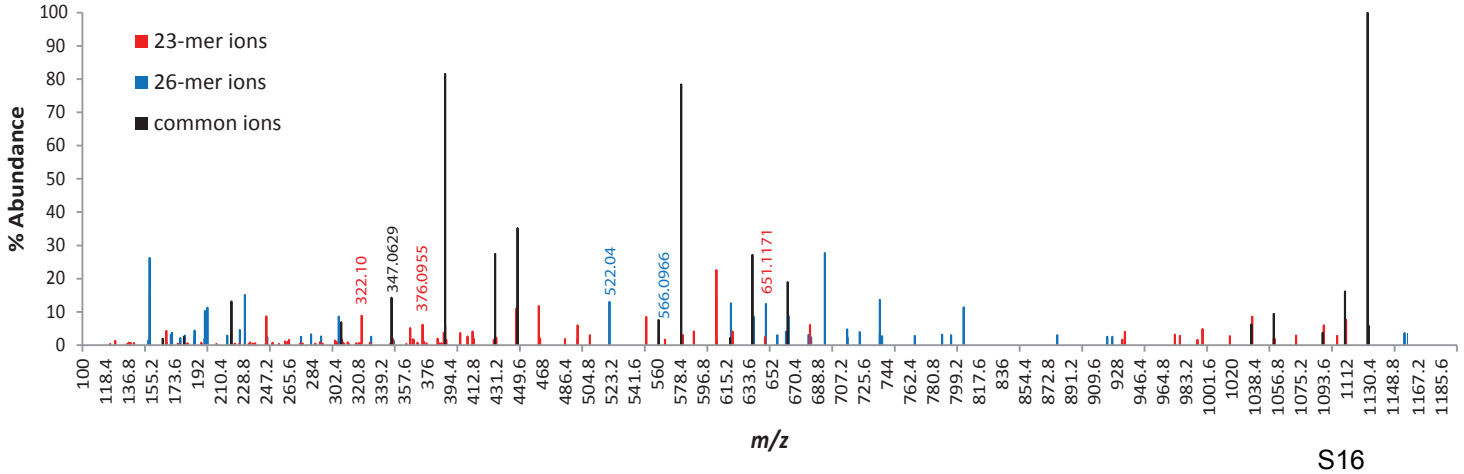

MS/MS Figure 3 (continued): Significant fragments from *C9S* compounds.

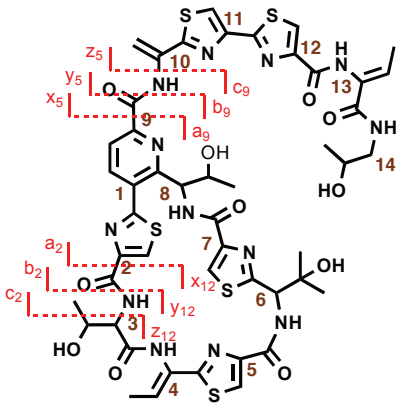

23-membered ring product
parent ion = 1146.2507

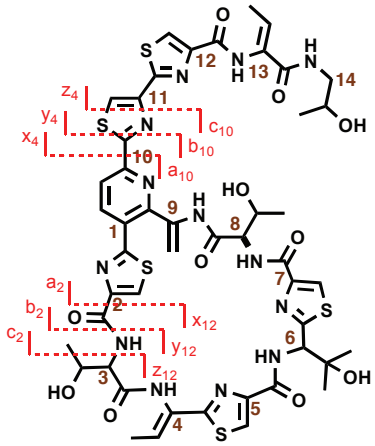

26-membered ring product
parent ion = 1146.2507

C9S 23-Membered ring product ms/ms data summary

Common Ions	Predicted	Diff (ppm)	Abund%	Ion
1129.2223	1129.2242	-1.7	6.41	M-NH2
1128.2423	1128.2402	1.9	100	M-H2O
1110.3118	1110.2960	14.2	18.54	M-2H2O
1092.2165	1092.2190	-2.3	4.05	M-3H2O
1053.1764	1053.1718	4.4	8.77	b13-H2O
1035.1593	1035.1612	-1.8	6.52	b13-2H2O
664.1079	664.1101	-3.3	6.58	b2-b7
636.1186	636.1152	5.3	17.81	b2-b7-CO
579.0794	579.0806	-2.1	5.83	a3-b7-b12-H2O
561.0424	561.0701	-49.3	1.11	a3-b7-b12-2H2O
448.1134	448.1108	5.9	3.11	y12-y7-H2O
430.1009	430.1002	1.6	17.53	y12-y7-2H2O
390.0692	390.0689	0.7	7.33	y11-z7-H2O
347.0629	347.0631	-0.5	3	y11-y7-H2O
181.0395	181.0430	-19.4	1.61	y9-y8-H2O
Unique Ions	**Predicted**	**Diff (ppm)**	**Abund%**	**Ion**
1102.2314	1102.2371	-5.2	10.25	M-CONH2
1100.2426	1100.2453	-2.4	11.3	M-CO-H2O
1070.1914	1070.1983	-6.4	15.13	c13-H2O
681.1327	681.1241	12.6	12.58	c9-z9-x8-H2O
663.1226	663.1135	13.7	8.55	c9-z9-x8-2H2O
651.1171	651.1261	-13.8	12.45	c9-y12-b3-H2O
633.1221	633.1155	10.4	8.78	c9-y12-b3-2H2O
606.0653	606.0683	-4.9	27.72	b3-c7-z2-H2O
578.0743	578.0733	1.7	100	b3-c7-z2-H2O-CO
562.0502	562.0784	-50.2	13.59	a3-b7-y2-2H2O
495.0370	495.1142	-155.9	11.42	a1-b7-z1
376.0955	376.0896	15.6	2.5	y5-H2O

C9S 26-Membered ring product ms/ms data summary

Common Ions	Predicted	Diff (ppm)	Abund%	Ion
1129.2412	1129.2242	15.1	5.82	M-NH2
1128.2440	1128.2402	3.4	100	M-H2O
1110.2213	1110.2960	-67.3	16.18	M-2H2O
1092.1740	1092.2190	-41.2	3.7	M-3H2O
1053.1746	1053.1718	2.7	9.39	b13-H2O
1035.1596	1035.1612	-1.5	6.27	b13-2H2O
664.1092	664.1101	-1.4	18.9	b2-b7
636.1154	636.1152	0.3	27.2	b2-b7-CO
579.0578	579.0806	-39.4	78.38	a3-b7-b12-H2O
561.0841	561.0701	25.0	7.54	a3-b7-b12-2H2O
448.1103	448.1108	-1.0	35.16	y12-y7-H2O
430.1021	430.1002	4.4	27.43	y12-y7-2H2O
390.0693	390.0689	1.0	81.54	y11-z7-H2O
347.0630	347.0631	-0.3	14.32	y11-y7-H2O
181.0446	181.0430	8.8	2.5	y9-y8-H2O
Unique Ions	**Predicted**	**Diff (ppm)**	**Abund%**	**Ion**
1093.2072	1093.2031	3.8	5.96	M-2H2O-NH2
646.1034	646.0996	5.9	2.44	b2-c7-H2O
580.0649	580.0890	-41.5	3.05	b2-b8
566.0966	566.1850	-156.2	1.71	y12-z6-H2O
513.0498	513.1373	-170.6	4.72	y12-y6-3H2O
486.1031	486.1264	-48.0	1.88	z12-x6-2H2O
465.1357	465.1373	-3.5	11.72	y12-z7-H2O
447.1263	447.1268	-1.0	10.99	y12-z7-2H2O
365.0808	365.0737	19.6	1.61	y11-y8
364.0909	364.0896	3.5	1.76	y11-z8-H2O
247.0518	247.0410	43.7	8.68	a10-z12-b8

MS/MS Figure 4: Fragmentation of compounds from *S(9,10)* cultures.

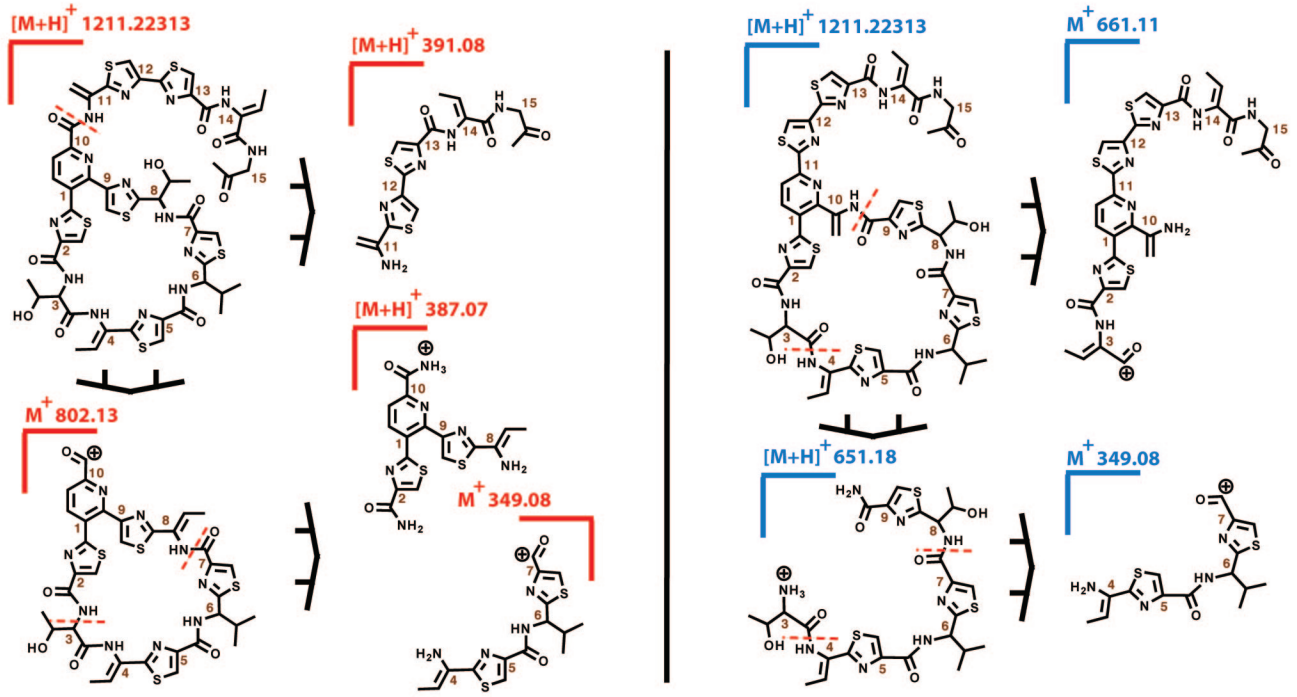

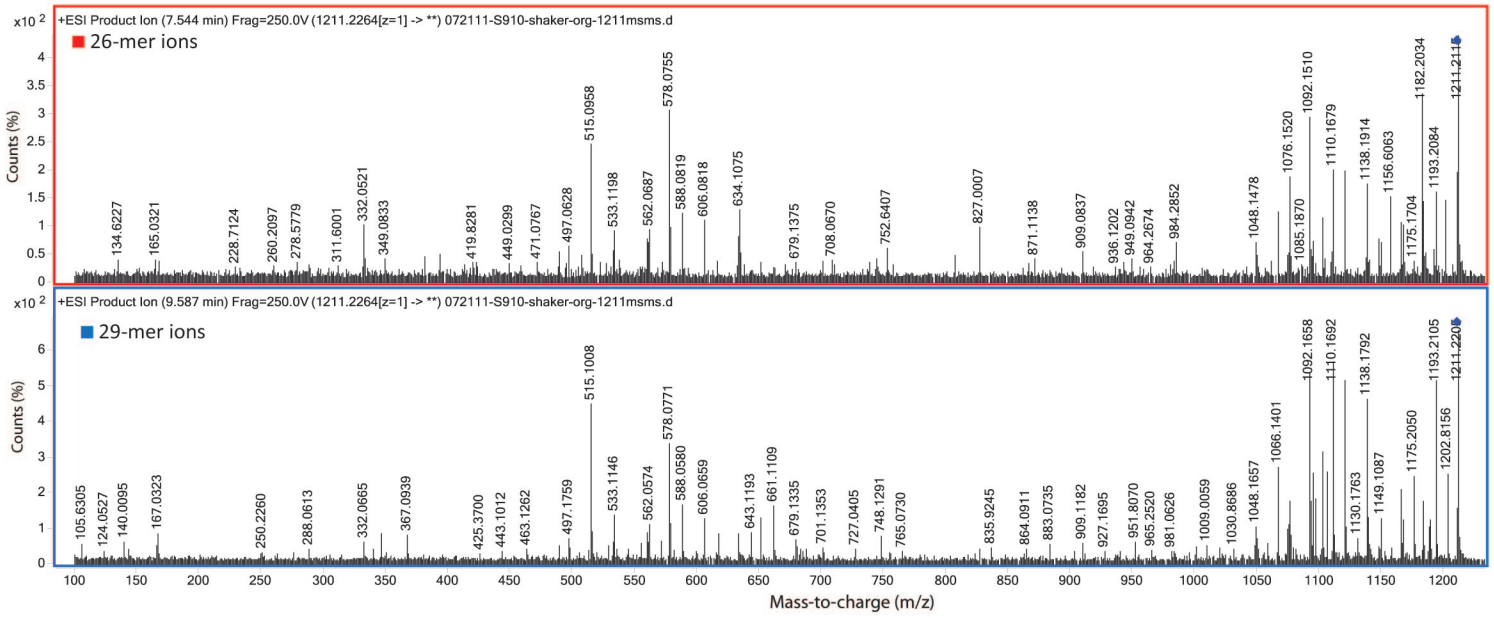

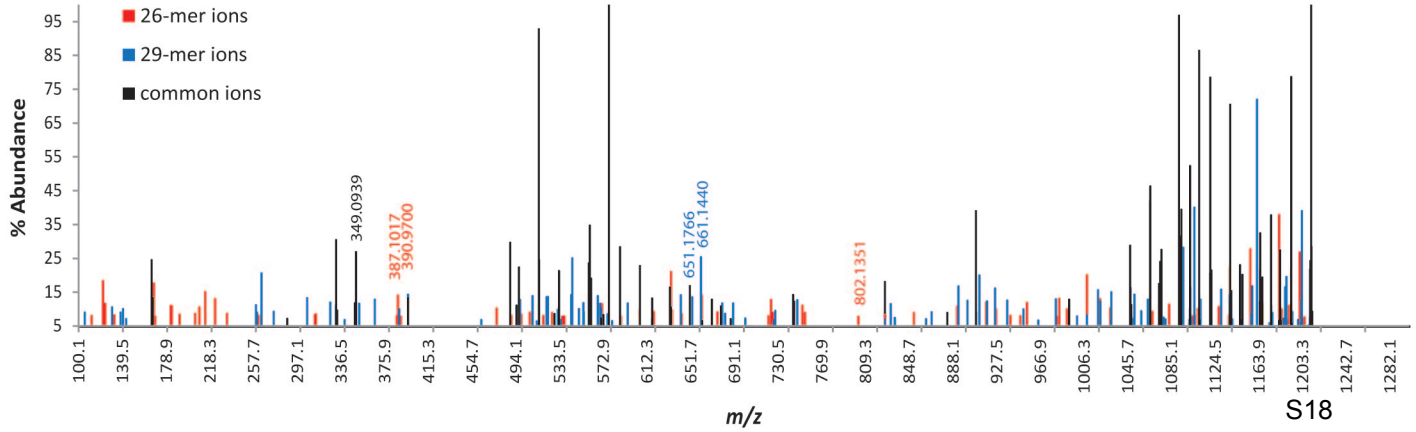

MS/MS Figure 4 (continued): Significant fragments from *S(9,10)* compounds.

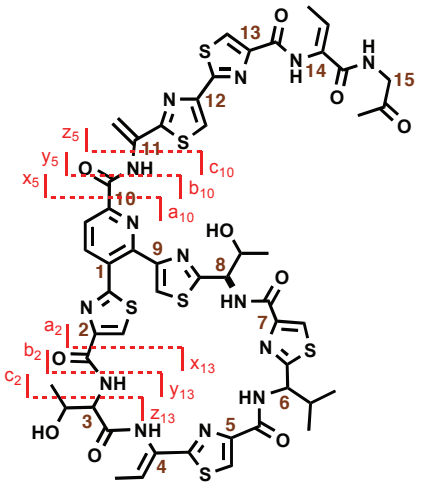

26-membered ring product
parent ion = 1211.2231

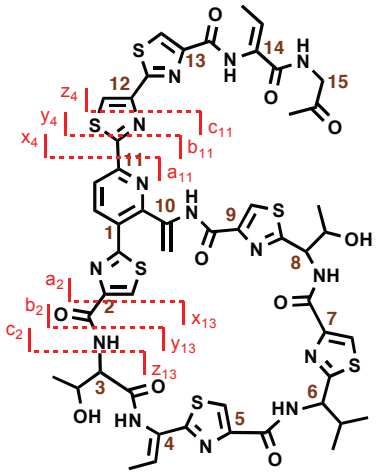

29-membered ring product
parent ion = 1211.2231

S(9,10) 26-Membered ring product ms/ms data summary

Common Ions	Predicted	Diff (ppm)	Abund%	Ion
1211.2360	1211.2231	10.6	100	M+H
1193.2284	1193.2126	13.3	78.7	M-H2O
1183.2347	1183.2282	5.5	27.43	M-CO
1175.2245	1175.2020	19.1	37.77	M-2H2O
1165.2463	1165.2177	24.6	32.43	M-CO-H2O
1147.2415	1147.2071	30.0	23.01	M-CO-2H2O
1139.0669	1139.1418	-65.8	15.36	b5-a6
1138.1916	1138.1704	18.7	70.49	b14
1121.2315	1121.1313	89.4	21.46	b5-a6-H2O
1120.1459	1120.1598	-12.4	78.51	b14-H2O
1110.1959	1110.1755	18.4	86.44	b2-b3
1102.1433	1102.1492	-5.4	52.33	b14-2H2O
1094.1435	1094.1567	-12.1	39.4	a2-c2-y1
1092.1112	1092.1649	-49.2	96.78	b2-b3-H2O
1076.1396	1076.1462	-6.1	27.56	a2-c2-y1-H2O
1066.1776	1066.1618	14.8	41.93	a2-c2-y1-CO
1048.1478	1048.1513	-3.3	28.83	a2-c2-y1-H2O-CO
1009.1302	1009.1819	-51.3	20.12	b3-b5-2H2O
993.1373	993.1506	-13.4	12.85	b5-b7-2H2O
909.1312	909.1421	-12.0	39.03	a12-2H2O
745.0770	745.0774	-0.6	12.26	b2-b7-NH3
744.1041	744.0934	14.4	14.28	b2-b7-H2O
687.9975	688.0672	-101.3	7.13	b2-b7-z1-H2O
679.1454	679.0907	80.6	10.8	a2-b7-z1
662.0455	662.0641	-28.2	6.53	a2-b7-y1
634.0261	634.0692	-68.0	10.46	a2-b7-x1
617.0496	617.0427	11.2	13.21	a2-b7-x1-NH3
606.0207	606.0141	10.9	22.77	c2-c7-y2
578.0309	578.0192	20.2	100	c2-c7-x2
562.0424	562.0047	67.1	19.07	b2-c7-x2
561.0444	561.0165	49.8	34.76	b2-b7-x2-H2O
350.1112	350.0502	174.3	26.84	x14-a5
349.0939	349.0787	43.4	11.76	y12-y8
332.0200	332.0396	-59.1	30.43	x14-a5-H2O
167.0323	167.0274	29.6	13.27	y12-y10
Unique Ions	**Predicted**	**Diff (ppm)**	**Abund%**	**Ion**
1109.1430	1109.1676	-22.2	10.04	a7-a8
982.0585	982.1710	-114.6	7.77	a3-c5-H2O
927.1751	927.1288	49.9	9.98	b2-c5
852.9714	853.0920	-141.4	8.95	c2-c5-y1-H2O
802.1351	802.1353	-0.2	7.76	b10-H2O
752.1407	752.1435	-3.7	11.09	c2-b3-z5
635.0753	635.1312	-88.0	9.73	c10-y12-b5-2H2O
618.9641	619.0999	-219.4	9.15	c10-b7-y10-2H2O
591.0614	591.1050	-73.7	3.45	c10-b7-y10-2H2O-CO
432.1027	432.1159	-30.5	3.11	y13-y8-H2O
390.9700	391.0767	-273.0	7.82	y5
388.1217	388.0533	176.3	14.06	c2-b7-z5-NH3
387.1017	387.0692	83.9	7.95	c2-b7-z5-H2O
314.0051	313.9927	39.6	8.52	c2-a8-y5
209.0356	209.0076	134.0	10.59	y5-x2
184.0512	184.0539	-14.7	10.97	y12-z10
183.0689	183.0587	55.9	11.05	y10-y8

S(9,10) 29-Membered ring product ms/ms data summary

Common Ions	Predicted	Diff (ppm)	Abund%	Ion
1211.2284	1211.2231	4.4	100	M+H
1193.2377	1193.2126	21.1	78.7	M-H2O
1183.2391	1183.2282	9.2	27.43	M-CO
1175.2486	1175.2020	39.6	37.77	M-2H2O
1165.2446	1165.2177	23.1	32.43	M-CO-H2O
1147.2298	1147.2071	19.8	23.01	M-CO-2H2O
1139.1175	1139.1418	-21.3	15.36	b5-a6
1138.2084	1138.1704	33.4	70.49	b14
1121.0994	1121.1313	-28.4	21.46	b5-a6-H2O
1120.1449	1120.1598	-13.3	78.51	b14-H2O
1110.1422	1110.1755	-30.0	86.44	b2-b3
1102.1437	1102.1492	-5.0	52.33	b14-2H2O
1094.1230	1094.1567	-30.8	39.4	a2-c2-y1
1092.1463	1092.1649	-17.0	96.78	b2-b3-H2O
1076.1176	1076.1462	-26.5	27.56	a2-c2-y1-H2O
1066.1401	1066.1618	-20.4	41.93	a2-c2-y1-CO
1048.1486	1048.1513	-2.5	28.83	a2-c2-y1-H2O-CO
1009.0059	1009.1819	-174.4	20.12	b3-b5-2H2O
993.1266	993.1506	-24.2	12.85	b5-b7-2H2O
909.1302	909.1421	-13.1	39.03	a12-2H2O
745.1009	745.0774	31.5	12.26	b2-b7-NH3
744.1411	744.0934	64.1	14.28	b2-b7-H2O
688.0063	688.0672	-88.5	7.13	b2-b7-z1-H2O
679.1404	679.0907	73.2	10.8	a2-b7-z1
662.0710	662.0641	10.4	6.53	a2-b7-y1
634.1036	634.0692	54.2	10.46	a2-b7-x1
616.9718	617.0427	-114.9	13.21	a2-b7-x1-NH3
606.1223	606.0141	178.5	22.77	c2-c7-y2
578.1387	578.0192	206.7	100	c2-c7-x2
562.1115	562.0047	190.0	19.07	b2-c7-x2
561.0489	561.0165	57.8	34.76	b2-b7-x2-H2O
350.1040	350.0502	153.7	26.84	x14-a5
349.0700	349.0787	-25.0	11.76	y12-y8
332.1200	332.0396	242.0	30.43	x14-a5-H2O
167.0337	167.0274	38.0	13.27	y12-y10
Unique Ions	**Predicted**	**Diff (ppm)**	**Abund%**	**Ion**
1130.1781	1130.1805	-2.2	15.84	M-CONH2-2H2O
1111.1238	1111.1469	-20.8	12.89	a5-a6
1096.0451	1096.2019	-143.1	28.21	z8-b10
1078.1846	1078.1914	-6.3	7.5	z8-b10-H2O
981.1044	981.1870	-84.2	12.01	y6-y8-H2O-CO
965.2520	965.1557	99.8	6.68	y8-x10-2H2O-CO
926.1656	926.1686	-3.3	16.18	y9-x8-z1-H2O
869.1824	869.1346	55.0	9.11	c2-b3-z3-H2O
661.1440	661.1105	50.7	25.39	y6-y12-H2O
651.1766	651.1836	-10.8	12.53	c9-b2
532.1172	532.1254	-15.4	9.78	c9-b3-H2O
522.0428	522.0471	-8.3	13.56	b2-b9-z1
367.0939	367.0893	12.5	12.88	c9-c5
339.9240	340.1022	-524.3	6.81	a9-b5
140.0095	140.0706	-436.4	10.06	z2